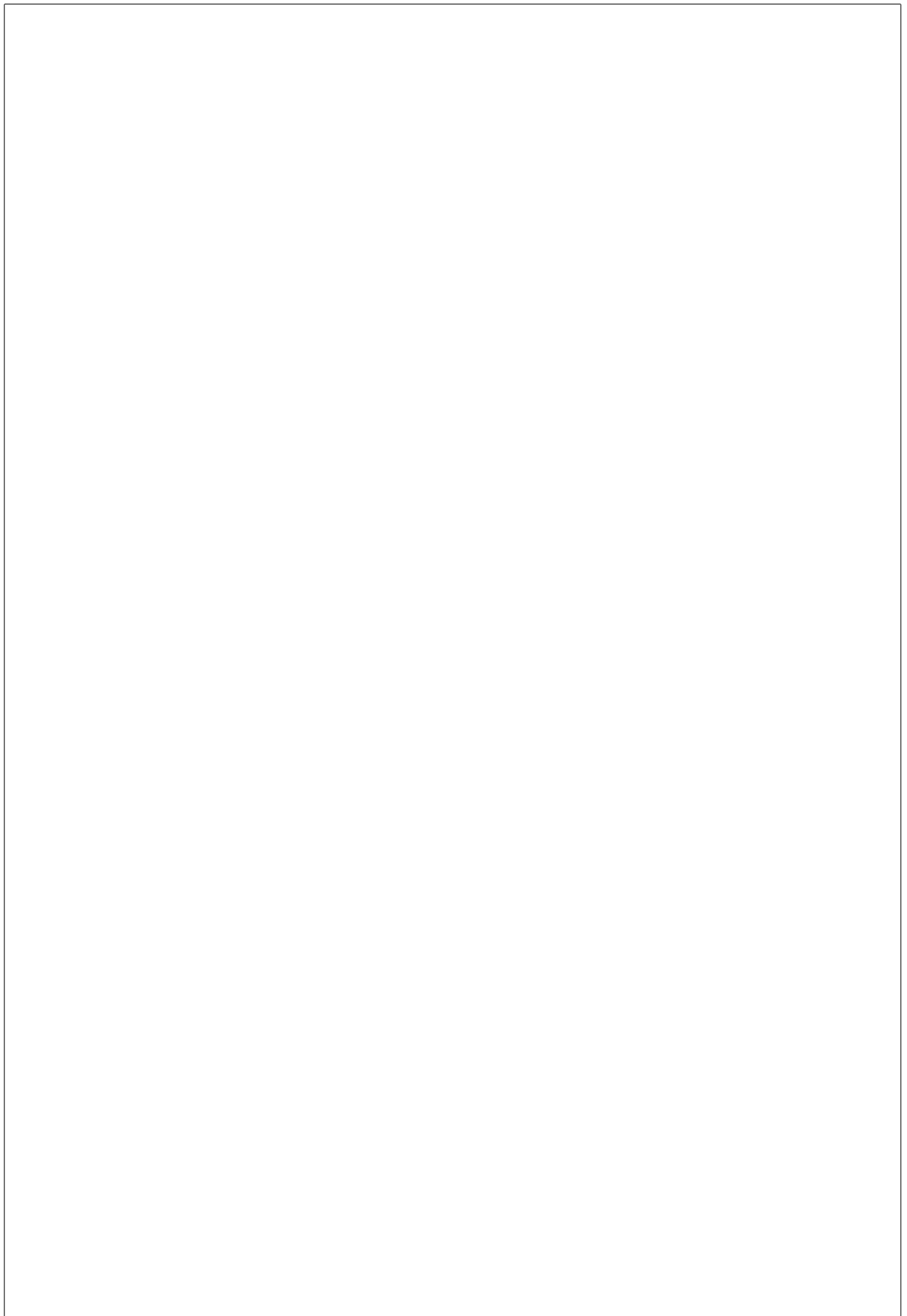


---

---



---

---

---

# Contents

<b>Table of Contents</b>	i
<b>List of Figures</b>	i
<b>List of Tables</b>	ii
0.1 Coupling Nanodiamonds to Optical Antennas . . . . .	1
0.1.1 Plasmonic Antennas . . . . .	1
0.2 Antennas . . . . .	3
0.2.1 Plasmonic Antennas . . . . .	6
0.2.2 Structure of the Plasmonic Antennas . . . . .	7
0.2.3 SiV center in a Plasmonic Double Bowtie Antenna . . . . .	9
<b>Index</b>	10

---

---

# List of Figures

1	Schematic of a double bowtie antenna . . . . .	2
2	Simul . . . . .	2
3	(a) Picture recorded with a commercial high resolution laser scanning microscope. The area shaded in blue represents the photoluminescence scan in image (b). (b) Photoluminescence scan of a 8 $\mu\text{m} \times 13 \mu\text{m}$ . . . . .	4
4	<caption> . . . . .	4
5	Image of the sample surface of 100 nm wet-milled nanodiamonds spin-coated on an iridium substrate illuminated with diffuse white light. The white bars are the horizontal bars of the cross markers which serve as a coarse orientation on the sample surface, the white dots are nanodiamonds, the big black spot is an artifact. . . . .	5
6	. . . . .	5
7	<caption> . . . . .	8
8	. . . . .	8
9	<caption> . . . . .	8
10	<caption> . . . . .	11
11	<caption> . . . . .	11
12	<caption> . . . . .	11
13	<caption> . . . . .	12
14	<caption> . . . . .	12
15	<caption> . . . . .	12

---

---

## List of Tables

---

## 0.1 Coupling Nanodiamonds to Double Bowtie Antenna Structures

Plasmonic nanoantennas are very recent devices designed to efficiently convert freely propagating optical radiation into localized energy and vice versa [?, ?, ?, ?, ?, ?]. Leveraging this unique property, integrating SiV centers with optical antennas creates coupled systems with a range of desirable features. These include enhanced photoluminescence emission and the ability to tailor photoluminescence spectra of the integrated emitters. The latter can be achieved by tuning the physical design parameters of the system including antenna geometry and emitter placement.

In this chapter we report on our efforts aimed at enhancing the properties of SiV centers by coupling them to optical double bowtie antennas. To this end we transfer selected nanodiamonds containing SiV centers to the target antenna structure using pick-and-place methods. After successful coupling we investigate the integrated structure experimentally. In addition to that we successfully relate some of our results to theoretical predictions.

In the following we give a short discussion of the most important properties of optical antennas. Then we sketch the actual coupling process and report on the optical properties of the resulting integrated structure.

### 0.1.1 Plasmonic Antennas

Optical nanoantennas act as converters between propagating and localized electro-magnetic fields. Thus, they can be used efficiently to couple photons in and out of nanoscale objects [?]. Due to their small physical sizes, comparable or smaller than the wavelength of visible light, they are capable of focusing optical fields to subdiffraction-limited volumes, offering the ability to manipulate electromagnetic fields at nanoscales [?, ?]. This property, dubbed sub-wavelength confinement, has successfully been exploited to enhance the excitation and emission of quantum emitters [?, ?, ?, ?] and to modify their spectra [?]. Resulting practical applications include near-field optical microscopy [?], surface enhanced spectroscopy [?, ?] and molecular sensing [?].

A nanoantenna is a nanostructure made from materials such as noble metals like gold or silver. These metals have in common that they are very susceptible to being polarized by electromagnetic fields. When illuminated by the incident electromagnetic radiation causes electrons in the metal to behave as a plasma that tends to move with respect to the atomic lattice. As a result excess charge at the opposite surfaces of the material accumulates and the material becomes temporarily polarized until restoring forces equilibrate the charge distribution.

Thus incident light of a given frequency induces oscillations in the free electron gas density in the surface layers of the metal. At resonance these light-induced oscillations exhibit modes of standing waves. The quasi-particles associated with these modes are known as localized surface plasmons (LSPs). For an in-depth treatment of LSPs in the context of nanoantennas we refer the reader to [?] and references therein.

Here it suffices to say, that LSPs facilitate the deciding property of optical antennas: Converting electromagnetic energy from the far-field into localized energy in the near-field. This

allows, in combination with the high collection-efficiencies of nanoantennas, to efficiently couple visible radiation with wavelengths of hundreds of nanometers, into small effective spatial volumes of only a few nanometer in diameter.

To create a controlled hot-spot several antenna designs are possible. In the context of this thesis we rely on double bowtie design available via a collaboration with N. Rahbany, group of C. Couteau, University of Technology of Troyes. ?? illustrates the typical bowtie antenna.

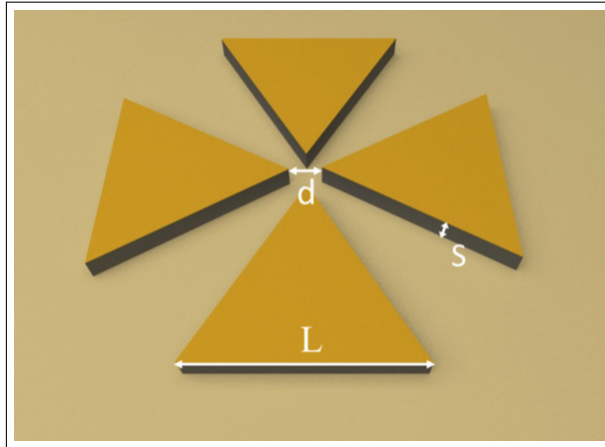


Figure 1: Schematic of a double bowtie antenna [?, ?].

This antenna design utilizing a symmetric arrangement of four identical triangle-shaped blocks, separated by a small gap. This setup allows LSP modes local to individual blocks to couple with each other resulting in the formation of an intense hot-spot in the center area [?], see ?. The actual electromagnetic response of a double bowtie nanoantenna depends on its physical design parameters such as gap size, material used, geometry and size. Furthermore, properties of incident light such as wavelength and polarization determine antenna operation.

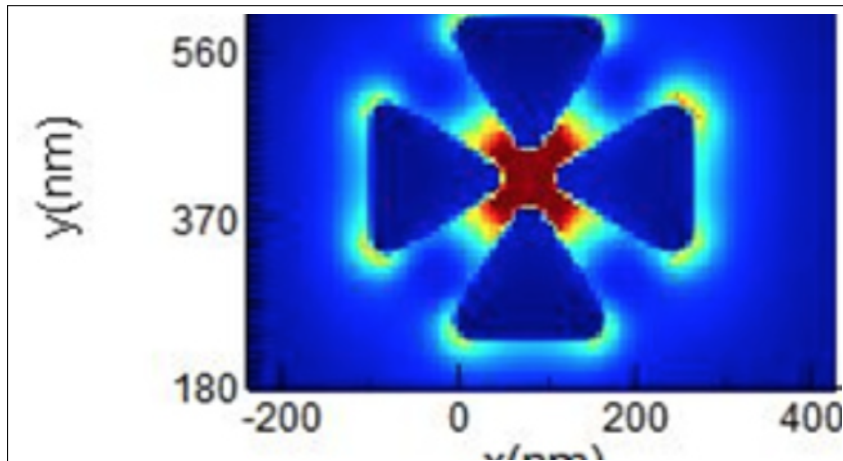


Figure 2: Simulation result of the electric field map of a gold double bowtie nanoantenna [?, ?]. The center of the antenna exhibits an area of pronounced focus.

The improved electromagnetic field at the center of a metallic nanoantenna can be used to

increase the spontaneous emission rate of emitters, a result known as Purcell effect [?]. The gap between the antenna arms acts as a resonant cavity providing a strong near field interaction with the emitter. This interaction modifies the density of states of the system, effectively providing additional modes for the emitter to decay into, thus amplifying its total decay rate. The amplification affects both radiative and non-radiative decay. The magnitude of the amplification for an emitter is quantified by the ratio of its enhanced decay rate to its free space decay rate, known as the Purcell factor  $F_p$ . This factor is proportional to  $Q/V_{eff}$  where  $Q$  denotes the quality of the antenna and  $V_{eff}$  the volume of the hot-spot. Thus antenna design must optimize  $F_p$  as a necessary condition for significant enhancement of fluorescence light emission.

In addition to the antennas local field enhancement, the emitters original quantum yield  $\eta_0$  influences the overall effectiveness of the emission enhancement. From theoretical considerations [?, ?, ?, ?], the modified quantum efficiency  $\eta$  of the combined system consisting of emitter and antenna can be obtained as

$$\eta = \frac{\eta_0}{\frac{1-\eta_0}{F_p} + \frac{\eta_0}{\eta_{ant}}}, \quad (1)$$

where  $\eta_{ant}$  denotes the fraction of fluorescence light which is not dissipated through losses in the metal of the antenna. It is clear that an emitter with  $\eta_0 \rightarrow 1$  will not profit from the Purcell effect. On the contrary, for realistic antennas with  $\eta_{ant} < 1$  antenna-induced losses reduce the overall quantum yield  $\eta$ . Consequently poor emitters with low initial  $\eta_0$  stand to profit the most from antenna-emitter coupling provided antennas are engineered well, i.e. they maximize their Purcell Factors and minimize their losses. For an in-depth review

The presented considerations illustrate that due to their relatively low quantum efficiency, SiV centers are excellent candidates for coupling with antennas. Thus it is promising to exploit the improved electromagnetic field at the center of a double bowtie antenna to enhance the spontaneous emission rate of SiV centers and thus improve their merit as single photon sources.

## 0.2 Coupling Nanodiamonds to Double Bowtie Antenna Structures

In this chapter, the integration of SiV centers in nanodiamonds with double bowtie nanoantenna structures is presented. The emission from the coupled system has two advantages:

- The antenna causes an enhancement in the SiV center's photoluminescence emission intensity.
- The photoluminescence spectrum of the nanodiamond is modified depending on the geometry of the nanoantenna as well as the position of the emitter in the gap. This provides the flexibility of designing the nanoantennas to accurately predict and tune the emitters' PL spectrum as desired.

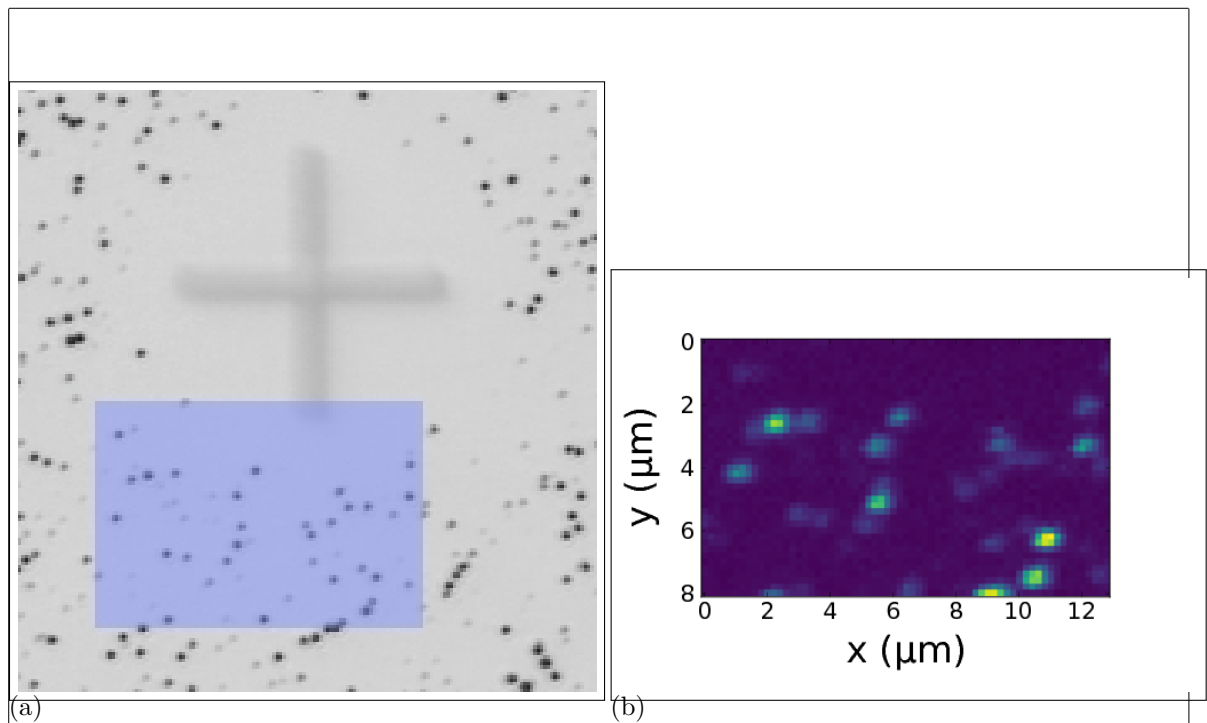


Figure 3: (a) Picture recorded with a commercial high resolution laser scanning microscope. The area shaded in blue represents the photoluminescence scan in image (b). (b) Photoluminescence scan of a  $8 \mu\text{m} \times 13 \mu\text{m}$

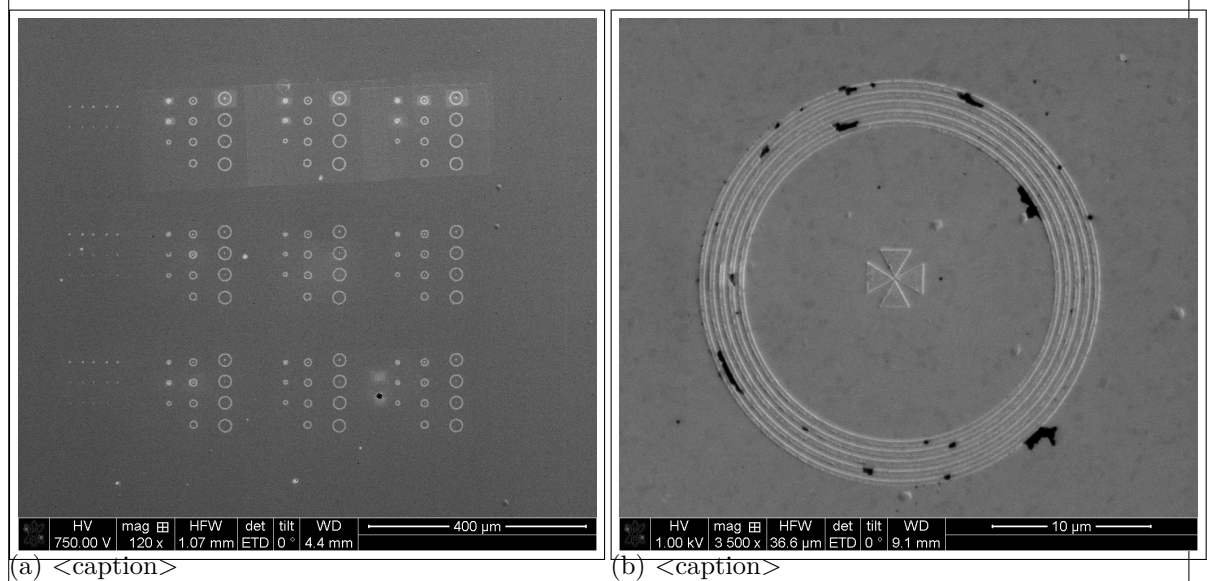


Figure 4: <caption>

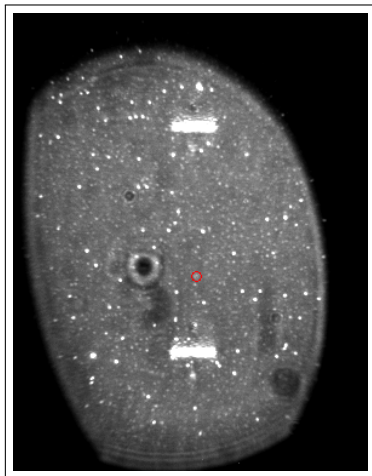


Figure 5: Image of the sample surface of 100 nm wet-milled nanodiamonds spin-coated on an iridium substrate illuminated with diffuse white light. The white bars are the horizontal bars of the cross markers which serve as a coarse orientation on the sample surface, the white dots are nanodiamonds, the big black spot is an artifact.

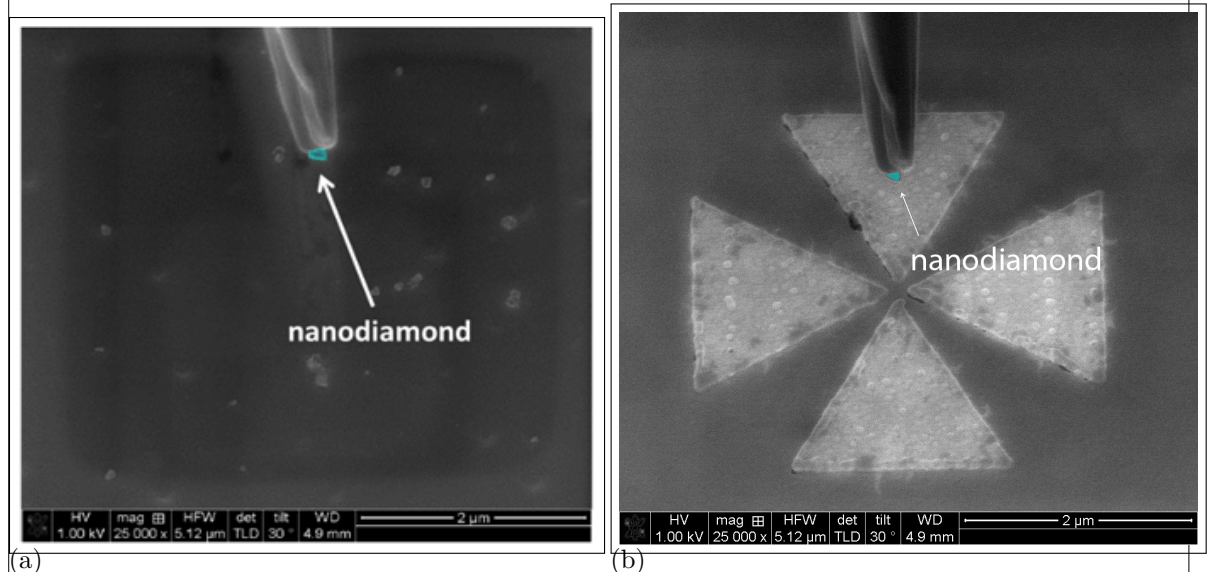


Figure 6

### 0.2.1 Plasmonic Antennas

[?] Optical antennas, acting as converters between propagating and localized fields, provide an effective route to couple photons in and out of nanoscale objects. These antennas are the counterparts of conventional radio and microwave antennas and operate in the visible regime (1, 2). Optical antennas have been shown to focus optical fields to subdiffraction-limited volumes (3), enhance the excitation and emission of quantum emitters (4–7), and modify their spectra (8).

A characteristic of antennas is their directed emission and reception. So far, the control of directionality has mainly been pursued by photonic crystal structures (9) and surface-plasmon-based devices (10–12). However, for such structures approaching the nanometer scale diffraction can limit the collimated beaming of light. On the other hand, the interaction of quantum emitters with light is best enhanced with microcavities (13, 14). Compared with these approaches, plasmonic nanoantennas offer a much smaller footprint in an open geometry combining strong subwavelength fields and increased transition rates, together with the prospect of directionality.

[?] from gold, a metal that can develop charge oscillations in its surface layers when excited by optical radiation. These antennas allow visible radiation, which has wavelengths of hundreds of nanometers, to couple into a semiconductor quantum dot only a few nanometers in diameter, and also direct the emission.

Good mode-matched antennas reradiate their energy after excitation within a single cycle of the wave. Molecules or quantum dots take nanoseconds or even longer to reradiate their energy. This time scale corresponds to about 1 million oscillations at optical frequencies, and the emission is in all directions.

If an atom, molecule, or quantum dot is placed into the near-field of a metallic nanoantenna (within about 1/50th the wavelength of the emitted radiation), its excited state can radiate photons very efficiently to free space (see the figure, panel B). The quantum emitters can emit a single photon, which can be exploited in quantum optics. Additionally, the nanoantenna can redirect radiation into a defined solid angle in space and impose a specific polarization on it.

The demonstration of the Purcell effect, which is the acceleration of the decay of the quantum emitter caused by impedance matching by the antenna to free space, could also enhance the radiative emission over nonradiative losses.

[?] The electro-magnetic antenna, originally referred to as an “aerial,” is a transducer between electromagnetic waves and electric currents, and generally operates in the radiofrequency regime. In analogy with the electro-magnetic antenna, we define the optical antenna as a device that converts freely propagating optical radiation into localized energy, and vice versa. The spatial extent of a receiver or transducer is commonly much smaller than the wavelength of radiation,  $\lambda$ , and is typically of the order of  $\lambda/100$ .

Surface plasmon resonances make optical antennas particularly efficient at selected frequencies. A generic antenna problem is illustrated in Fig. 3. It consists of a transmitter and a receiver, both represented by dipoles  $p$ . The antenna is introduced to enhance the transmission efficiency from the transmitter to the receiver. This enhancement can be achieved by increasing the total amount of radiation released by the transmitter, for which the antenna efficiency is a useful figure of merit:

$$p = p \quad (2)$$

where  $P$  is the total power dissipated by the antenna,  $P_{\text{rad}}$  is the radiated power and  $P_{\text{loss}}$  is the power dissipated through other means, such as by absorption in the antenna. However, the transmission efficiency can also be improved by directing the radiation in the direction of the receiver. The efficiency for this process is represented by the directivity:

$$p = p \quad (3)$$

where the angles  $\hat{\mathbf{y}}$  and  $\hat{\mathbf{T}}$  represent the direction of observation and  $p(\hat{\mathbf{y}}, \hat{\mathbf{T}})$  is the angular power density. The combination of antenna efficiency and directivity is referred to as the antenna gain:

$$p = p \quad (4)$$

By reciprocity, we can interchange the fields and sources in Fig. 3 to give  $p_1 \rightarrow E_2 = p_2 \rightarrow E_1$ , where  $E_1$  ( $E_2$ ) is the field of dipole  $p_1$  ( $p_2$ ) evaluated at the location of  $p_2$  ( $p_1$ ). A good transmitting antenna is therefore also a good receiving antenna. For a transmitter in the form of a two-state quantum emitter, reciprocity leads to a relationship between the emitter's excitation rate  $\dot{N}_{\text{exc}}$  and its spontaneous emission rate:

$$p = p \quad (5)$$

Here, the superscript  $\rightarrow$  refers to the absence of the antenna and the subscript  $\hat{\mathbf{y}}$  indicates the polarization state; that is, the electric field vector points in direction of the  $\hat{\mathbf{y}}$  unit vector. An equivalent equation holds for polarization in the  $\hat{\mathbf{T}}$  direction. Interestingly, excitation in a direction of high directivity allows the excitation rate to be enhanced more strongly than the radiative rate. Another important antenna parameter is the antenna aperture, which is formally the same as the absorption cross-section sigma. Let us consider a dipole-like receiver with a cross-section  $\dot{N}_0$  that is not coupled to an antenna. The unit vector in the direction of the absorption dipole axis is denoted as  $\hat{\mathbf{n}}$  and the incident field at the location of the receiver is  $E_0$ . Once we couple the receiver to an antenna, the field at the receiver increases to  $E$  and the cross-section or antenna aperture becomes

$$p = p \quad (6)$$

Thus, the aperture of an optical antenna scales with the local intensity enhancement factor. Theoretical and experimental studies have shown that intensity enhancements of  $10^4$ – $10^6$  are readily achievable<sup>14,36,37</sup> and hence, for typical molecules with free-space cross-sections of  $\sigma_0 = 1 \text{ nm}^2$ , we find that a layer of molecules spaced  $0.1 \text{ nm}$  apart can absorb all of the incident radiation if each molecule is coupled to an optical antenna. Of course, this estimate ignores the coupling between antennas and therefore has limited validity.

### 0.2.2 Structure of the Plasmonic Antennas

FDTD numerical simulations were performed using Lumerical software to characterize gold double bowtie nanoantennas on a gold substrate. The nanoantennas are tailored to have a gap of  $g = 150 \text{ nm}$  (taking into account the diameter of the nanodiamonds of around  $100 \text{ nm}$ ), side length of  $L = 2 \mu\text{m}$ , and a thickness of  $t = 60 \text{ nm}$  (see Fig. 3a). Upon excitation with incident light, an intense electromagnetic hotspot is formed in the nanoantenna gap [?], which is expected to excite a nanodiamond containing SIV centers aiming to enhance its fluorescence emission. Unlike a single bowtie that is sensitive only to the polarization along its principle axis

read paper

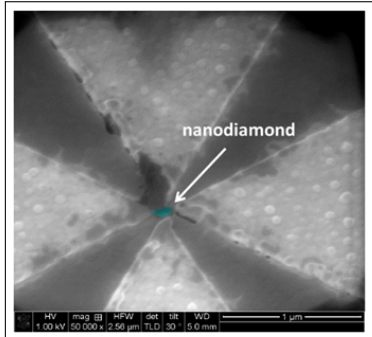


Figure 7: &lt;caption&gt;

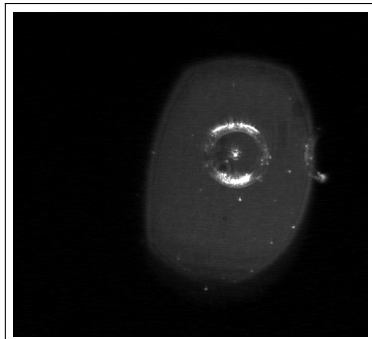


Figure 8

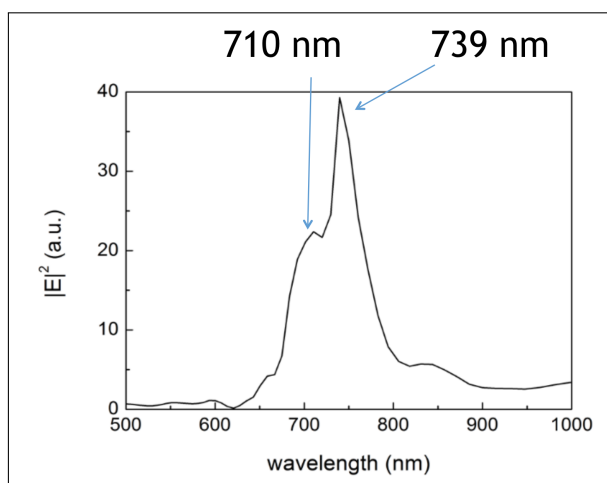


Figure 9: &lt;caption&gt;

(C2 rotational symmetry), a double bowtie features a C4 rotational symmetry and therefore focuses both parallel and perpendicular polarizations (i.e. all in-plane directions). The index of refraction of gold is taken from Palik [1], and that of the nanodiamond is chosen to be  $n = 2.4$  at  $\lambda = 660\text{ nm}$ . The electric field intensity in the nanoantenna gap is then measured as a function of wavelength to identify the antenna resonance. The spectrum is given in Fig.3b where we observe that the resonance shows two peaks; an intense peak coinciding with the SiV emission wavelength ( $\lambda = 739\text{ nm}$ ), and an additional mode at a lower wavelength ( $\lambda = 710\text{ nm}$ ) [?]. The resonance spectrum of the antenna alone shows only one peak at 739 nm. Thus, the additional peak is attributed to the presence of the nanodiamond that is slightly shifted from the center of the gap, corresponding to our experimental conditions. These calculations suggest, that the emission from an SiV center at 738 nm is effectively enhanced and directed by the antenna.

Palik, E.  
D. Handbook of optical constants of solids.  
3, (Academic press, 1998)

### 0.2.3 SiV center in a Plasmonic Double Bowtie Antenna

In the following, specific details and challenges concerning the coupling process are given and results of the spectroscopic measurements of an SiV center in a plasmonic double bowtie antenna are reported.

We performed coupling the nanodiamonds containing SiV centers in two approaches: First we chose a nanodiamond containing several SiV centers for pick-and-place and afterwards a nanodiamond containing a single SiV center. As mentioned before, single SiV centers may be damaged by the electron radiation in the SEM during pick-and-place and stop emitting photoluminescence light. Hence, we decided to run first experiments with nanodiamonds containing multiple SiV centers. This approach has the advantages that we are able to gain experience in the execution of the pick-and-place process without the risk of permanently damaging the emitter and therefore rendering the tedious pick-and-place process futile. For measurements of the intensity enhancement by the antenna, a single emitter is necessary. However, the antenna's influence on the SiV center spectrum can be studied when several emitters are present. Therefore, studies of the spectrum are performed in this first approach.

After we gained experience with the first approach, we searched for a suited nanodiamond containing a single SiV center. The aim was to perform saturation and second order correlation measurements to probe single SiV centers, and consequently quantify the exact Purcell enhancement imposed by the nanoantenna on a single photon emitter.

### Nanodiamond With Multiple SiV centers Coupled to Antenna

The nanodiamonds exploited for the approach of coupling multiple SiV centers to an antenna were produced by a wet-milling process from a CVD diamond film<sup>1</sup>. The solution of nanodiamonds which exhibit a median size of 100 nm were spin-coated on an iridium substrate treated with Piranha etch. To ensure that a pre-characterized nanodiamond exhibiting preferred optical properties (eg. narrow linewidth, high count rate) is later found again, the iridium substrate was engraved with reference cross markers produced by a focused ion beam prior to the spin-coating process. After spin-coating, the sample was placed in an oven for 3 hours at 450 °C to oxidize the surface and remove any residual graphite and amorphous

<sup>1</sup>wet-milling performed by A. Muzha, group of A. Krueger, Julius-Maximilians Universität Würzburg, diamond film grown by group of O. Williams, School of Engineering, Cardiff University

carbon.

?? shows the spectrum recorded of the preselected nanodiamond. The ZPL peak exhibits a wavelength of 738.55(1) nm and a linewidth of 5.00(3) nm. These numbers correspond well to the ZPL of unstrained SiV centers and therefore allows us to deduce that the studied nanodiamond contains at least one SiV center. Photon autocorrelation measurements revealed, that the nanodiamond contains multiple SiV centers.

To determine the position of the nanodiamond on the original substrate, first a scan with a commercial laser scanning microscope (LSM) was performed as described in ???. ?? shows a part of an obtained LSM image. The cross marker can easily be identified, the black dots are nanodiamonds. After transferring the sample into the confocal setup, confocal scans of the corresponding areas are performed (??). The area corresponding to the fluorescence light scan in ?? is shaded blue in ???. When looking closely, the bright spots in the fluorescence light scan can be identified with nanodiamonds visible in ???. The image in the SEM is very similar to the image obtained by the LSM. Therefore, once a nanodiamond containing a preselected emitter is identified in the LSM scan, it is easy to find the same emitter in the SEM.

The picking part of the pick-and-place process was performed in the same manner as described in the section about VCSELs (??). The gold surface of the plasmonic antenna caused a high adhesion between the antenna surface and the nanodiamond. Once the nanodiamond touched the gold, it could not be picked up again with the tungsten tip. The nanodiamond first touched the antenna structure a few nanometers away from the gap and immediately stucked to the surface, on top of one of the triangles. Therefore, the nanodiamond had to be pushed into the gap with the nanomanipulator tip. This process caused some damage to the antenna structure. The damage is visible as black area at the tip of the top triangle in ???. However, FDTD simulations of damaged antennas reveal that this modification of the antenna hardly influences the antenna resonance.

After this deterministic placement we measure the PL spectrum of the nanodiamond to identify the effect of the nanoantenna on its emission. The result is displayed in ???. The additional peak at a lower wavelength is attributed to the antenna resonance mode. To verify this, we convolute the experimental PL spectrum of the nanodiamond measured before placing it in the nanoantenna (??) with the intensity spectrum of the nanoantenna obtained by simulations (??). The resulting spectrum is given in ???, and is in good agreement with the measured spectrum in ???, confirming that indeed the extra peak is due to the antenna resonance.

### Nanodiamond With Single SiV center Coupled to Antenna

sample M02-16: drop-casted with SiGH45 First, only a small percentage of the technically suited nanodiamonds (size, isolation) contain a single SiV center, second, damage due to electron radiation during pick-and-place. After an SiV center with a small dig in the  $g^{(2)}$  function, indicating only few SiV centers.

fehlergrenzen  
verfuenftig  
machen

bild dazu

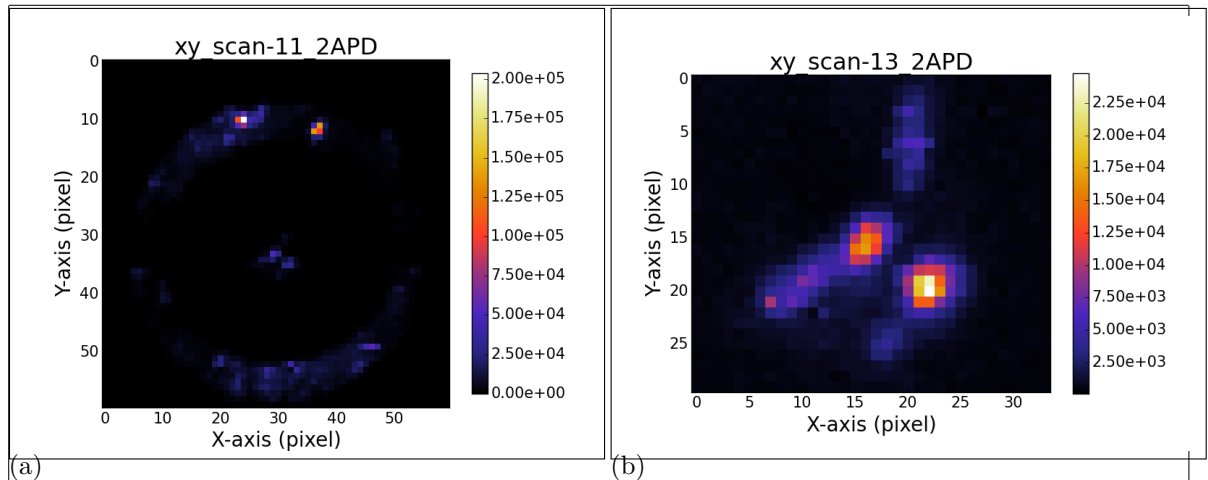


Figure 10: &lt;caption&gt;

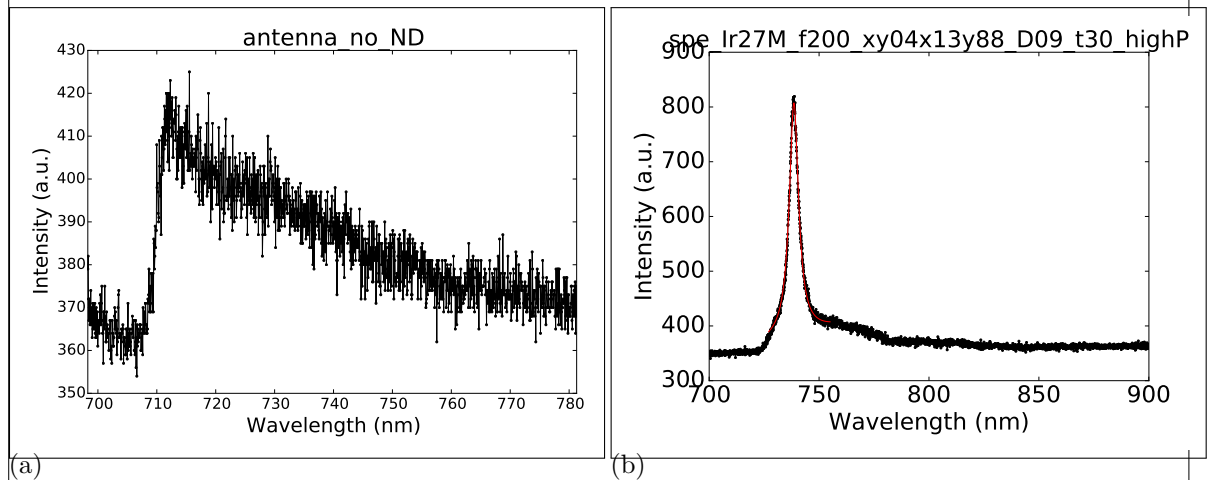


Figure 11: &lt;caption&gt;

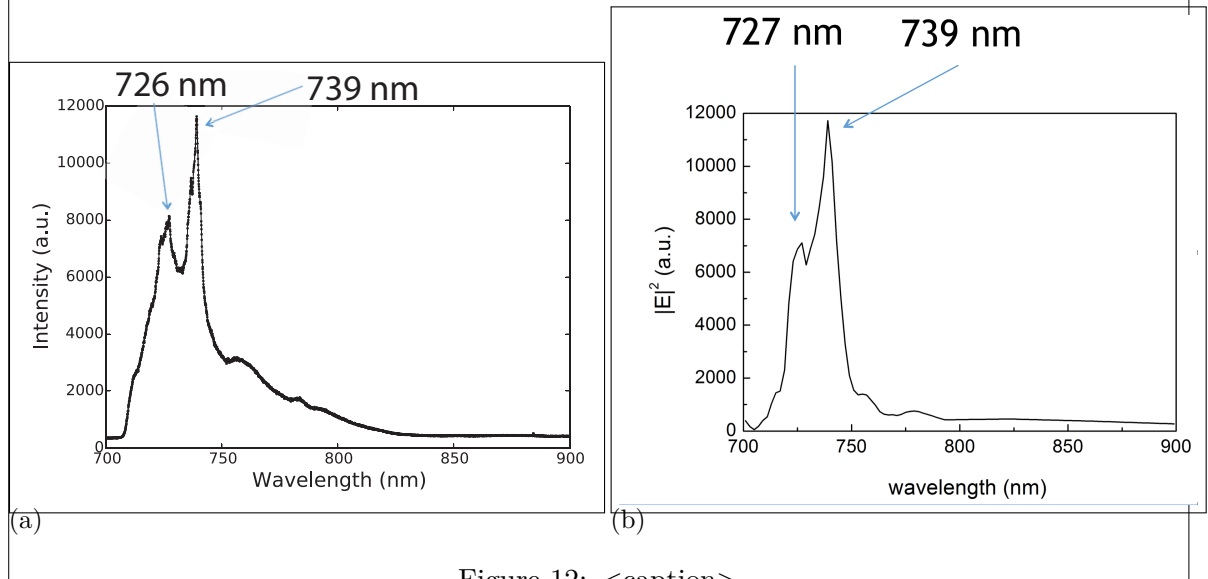


Figure 12: &lt;caption&gt;

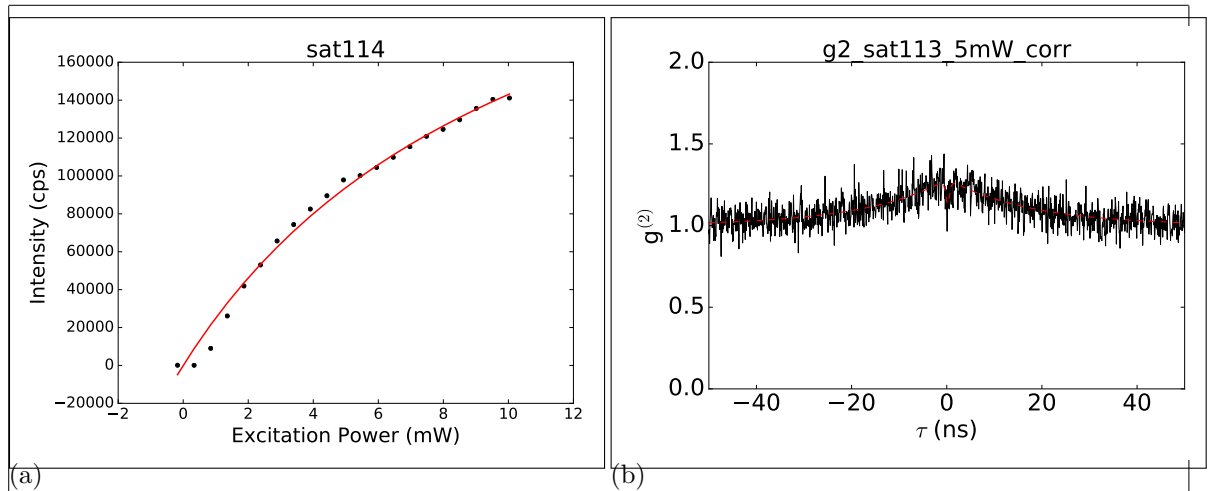


Figure 13: &lt;caption&gt;

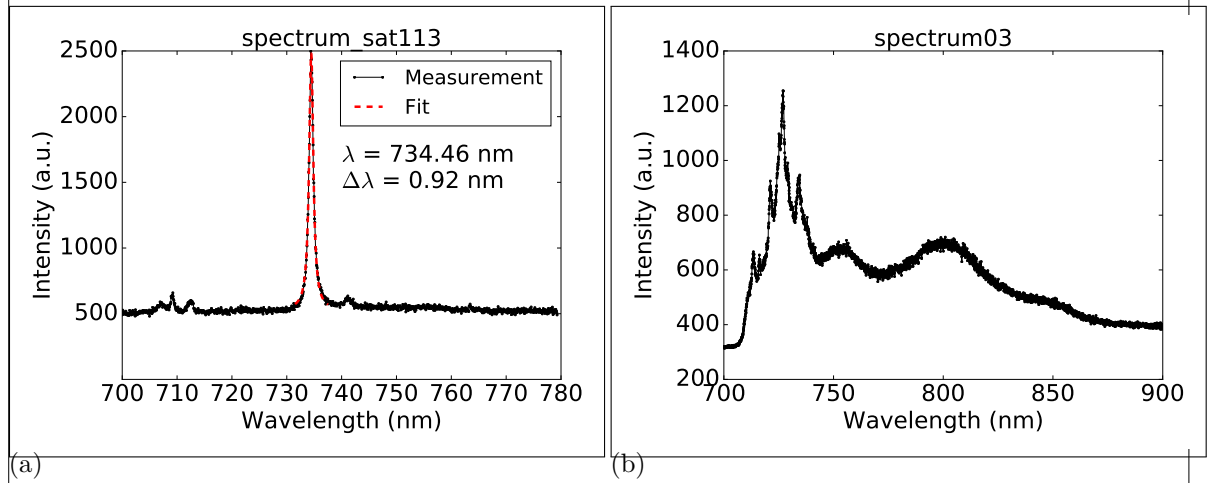


Figure 14: &lt;caption&gt;

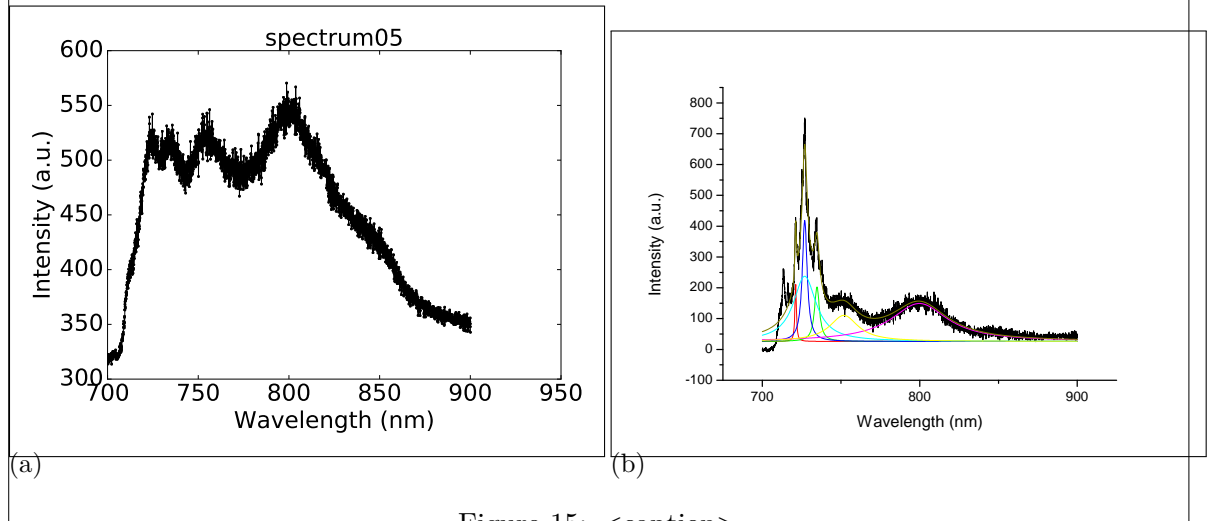


Figure 15: &lt;caption&gt;